Clays and Clay Minerals, Vol. 24, pp. 320–326. Pergamon Press 1976. Printed in Great Britain

SURFACE CHARGE VARIATION IN AGING FERRIC HYDROXIDE

R. W. LAHANN

Department of Geological Sciences, State University of New York at Binghamton, Binghamton, NY 13901, U.S.A.

(*Received* 30 *January* 1976; *and in final form* 29 *June* 1976)

Abstract—The variation with time of exchangeable surface charge of amorphous ferric hydroxide in aqueous suspension was monitored by a titration technique. After 120 days, the surface charge of suspensions with initial pH from 8.5 to 10.5 was about one-fourth of the initial value, and goethite had formed from the ferric hydroxide. After the same time interval, the exchangeable surface charge of suspensions with initial pH from 5.5 to 8.0 was about two thirds the original value and the ferric hydroxide was still largely amorphous. The initial rate of crystallization and surface charge reduction increased with initial pH for suspensions with pH from 8.5 to 10.5, whereas the rate of surface charge reduction appeared to be independent of pH for suspensions with initial pH between 5.5 and 8.0. Based on these results it is suggested that at pH from 8.5 to 10.5 ferric hydroxide ages to goethite via a solution stage involving the $Fe(OH)_4^-$ ion, whereas at pH values below 8.5 ferric hydroxide aging proceeds via mechanisms which do not involve the particle surface or bulk solution.

INTRODUCTION

Ferric hydroxides are known to occur in soils and sediments as discrete particles and as coatings on other particles. The most common crystalline forms of iron oxide in nature are hematite (α-Fe_2O_3) and goethite (α-FeOOH), although maghemite (β-Fe_2O_3) and lepidocrocite (β-FeOOH) are also found. Amorphous hydrated iron oxide and mixtures of crystalline material with it are often observed (Schwertmann and Fischer, 1973; Fischer and Schwertmann, 1975). Many workers (Mackenzie, 1957; Schellman, 1959; Gastuche *et al.*, 1964; Schwertmann, 1969; Landa and Gast, 1973) have shown that hematite, goethite, or both may form with time from amorphous ferric hydroxide. Rate of crystallization and crystalline species formed are influenced by several variables. Crystallization rate is enhanced by dialysis (Gastuche *et al.*, 1964), washing of the sample (Schellman, 1959), and high solution pH (Mackenzie and Meldau, 1959). Hematite formation is favored by low or neutral pH (Schellman, 1959; Schwertmann, 1969), preheating of the sample, increasing temperature, and increasing suspension concentration (Schwertmann and Fischer, 1966), whereas goethite formation is favored by high pH (Schellman, 1959; MacKenzie and Meldau, 1959).

Gastuche (1964); and Fripiat and Pennequin (1965) suggested that a ferric hydroxide precipitate may pass through three stages with time: 1. flocculation, 2. deflocculation, and 3. polymerization–crystallization. Gastuche (1964) reported that maximum deflocculation of a dialyzed ferric hydroxide gel occurred 6–8 days after precipitation, whereas Fripiat and Pennequin (1964) reported that particles of a dialyzed ferric hydroxide gel had minimum molecular weight 2–3 days after precipitation. In both of the above studies, the authors noted that ferric hydroxide gels in acidic solution experienced deflocculation, whereas identical gels in basic medium did not. Fripiat and Pennequin (1965) suggested that acidic ferric gels deflocculate because of the mutual repulsion of positively charged particles.

The sign of the charge developed on a ferric oxide particle at a particular pH is a function of composition, structure, and sample history. Parks and DeBruyn (1962) defined the zero-point-of-charge (zpc) for a material as the pH value at which the net surface charge on the particles in an aqueous suspension is zero. Parks (1965) tabulated from the literature a large number of zpc determinations for ferric oxides and hydroxides. Reported zpc values ranged from 3.2 to 7.2 for goethite and 4.3–8.8 for amorphous iron oxide. Low zpc values were generally associated with natural samples or dried synthetic samples.

The total surface charge developed by a material at a specified pH and electrolyte concentration is a function of surface area. Gastuche (1964) stated that a ferric hydroxide gel maintained at low pH has initially a low surface area, which then increases in response to deflocculation, only to decrease again because of polymerization. The surface area of a ferric hydroxide gel maintained at high pH would presumably only decrease with time as polymerization and crystallization took place.

The surface chemistry of ferric hydroxide particles may be inferred from studies on ferric oxides. The nature of the interface between ferric oxide and aqueous solution was investigated by Parks and DeBruyn (1962); and by Atkinson *et al.* (1967). These studies concluded that, in the absence of other adsorbed species, ferric oxide particles vary surface charge by bonding protons from the liquid onto surface hydroxyls as pH is lowered, and conversely by

https://doi.org/10.1346/CCMN.1976.0240608 Published online by Cambridge University Press

desorbing protons from surface hydroxyl groups as pH increases. The theory of proton adsorption isotherms was discussed by Parks (1967) and the effect of electrolyte concentration on such adsorption was demonstrated by Atkinson *et al.* (1967) who showed that proton adsorption or desorption by ferric oxide suspended in 1 N KCl was a linear function of the pH variation produced by adding HCl. If ferric hydroxide particles vary surface charge in the same manner as ferric oxide, proton adsorption in 1 N KCl should be an approximately linear function of pH. The slope of the adsorption isotherm would then be a measure of the surface area of the suspended solid, and as such could be used to indicate the degree of deflocculation or crystallization which has occurred in the gel. This procedure has several advantages over N_2 gas adsorption surface area determinations. Most important, an indication of surface area change may be obtained through use of commonly available laboratory equipment and the measurement may be made without heating and drying the sample, two processes known to promote hematite crystallization (Schwertmann and Fisher, 1966).

The work of MacKenzie and Meldau (1959) and Schellman (1959) indicate that solution pH may influence both the rate of crystallization and the crystallization product. Solution pH may, in turn, be influenced by processes taking place within an ageing gel. Specifically, ion exchange reactions and decrease in gel surface area may result in release of protons or hydroxyl groups to the bulk solution. If some of the iron atoms in a ferric hydroxide precipitate are coordinated to ions other than OH^- (e.g. Cl^-, SO_4^{-2}) then replacement of the foreign ion by OH^- as crystallization proceeds (expulsion of the foreign ion from the growing crystal) will result in a decline in solution pH because of extraction of OH^- from the solution. The probable effect of surface area reduction on bulk solution pH is dependent on the sign of the charge on the particles. If the surface charge is negative, surface area reduction should release hydroxyl units and raise the solution pH. Alternatively, if the surface charge is positive, surface area reduction should lower the solution pH and reduction of the area of a neutral surface should have little effect on solution pH.

While it is impossible, because of the complexity of the system, to predict the pH variation with time of a solution in contact with an aging ferric hydroxide gel, it is possible to predict how the solution pH variation will effect the slope of the adsorption isotherms. If the solution pH is such that the particles are continually within the pH region of either negative, neutral, or positive surface charge, one would predict a continuous, progressive, reduction in adsorption slope as crystallization occurs. If, however, the solution pH is lowered so as to change the surface charge from negative to positive (because of hydroxyl uptake by the gel) one would predict that in the pH region of the zpc the adsorption slope would approach a minimum because of increased particle associations and that as surface charge increased, after passing through the zpc, increased particle repulsions, as suggested by Fripiat and Pennequin (1965), should result in an increase in the adsorption slope.

The goal of the present study was to test the following hypotheses:

1. that variation in the slope of a proton adsorption isotherm for ferric hydroxide suspended in 1 N KCl may be used to indicate crystallization within the gel;
2. that variation in the slope of the proton adsorption isotherm may be used to measure the differences in crystallization rate as a function of solution pH;
3. that changes in proton adsorption slope with time may be predicted on the basis of variation of surface charge of the solid.

EXPERIMENTAL

Preparation of ferric hydroxide gel

Two-liter volumes of solution, each containing sufficient Fe to give 8 g of $Fe(OH)_3$, were prepared with initial pH values of 4.5, 5.5, 6.5, 7.5, 8.0, 8.5, 9.0, 9.5, 10.0 and 10.5. The first step in this procedure involved dissolving 20.234 g of $FeCl_3 \cdot 6H_2O$ in 800 ml of distilled water. The pH of this ferric chloride solution was brought to about 12 by stirring continuously during the addition of eight 40-ml aliquots of 1 N KOH at 2 min intervals. The suspension pH was adjusted to the desired value by adding 2 N HCl, and the total volume was brought to 2 liters by adding distilled water. The suspension was remixed, the pH was recorded, and 250-ml samples containing both fluid and suspended solid were extracted after elapsed times of 1, 2, 4, 7, 15, 30, 60, and 120 days. By extracting both solid and fluid simultaneously, an analysis can be made without altering the activities of any species in the system.

pH measurement

pH was measured by feeding the output from a Beckman 39301 glass electrode and a Corning 476109 calomel electrode through a Cary vibrating reed electrometer which was interfaced with a Leeds and Northrup 7554 Type K-4 potentiometer. Reproducibility of ± 0.01 pH units was possible with this instrument.

Surface charge measurements

The surface-charge measurement method of Parks and DeBruyn (1962) was used. One gram of $Fe(OH)_3$ was suspended in 250 ml of 1 N KCl in a glass beaker at 22°C ± 2°C. The solution pH was adjusted to a value near 10 by addition of 1 N KOH. A series of 0.5 ml aliquots of 0.30 N HCl were added to the suspension and pH change recorded. When a solution pH of about 4 was reached, the suspension was titrated in the reverse direction with 0.30 N KOH. Titrations were followed by feeding the output of the Cary vibrating reed electrometer to a strip-chart

https://doi.org/10.1346/CCMN.1976.0240608 Published online by Cambridge University Press

recorder. Addition of KOH reversed, within 0.05 pH units, the results of acid addition. The largest volume of titrant added in any experiment was 5 ml, too small an amount to significantly change the ionic strength of the suspension.

Adsorption of bicarbonate ions onto ferric hydroxide at low pH would be predicted based on the work of Hingston *et al.* (1968). Since the results for titration of duplicate samples under N_2 gas and under normal atmosphere were not significantly different, it was concluded that the CO_2 adsorption by the suspension was not great enough to require operating under the N_2 atmosphere.

Differences between calculated and observed pH changes allow calculation of proton adsorption and desorption by the suspended oxide. Linear regression slopes and correlation coefficients for proton adsorption as a function of pH were calculated for all materials titrated in this study. Analysis of duplicate samples indicated the adsorption slopes were reproducible to within about 1×10^2 μmoles/g·pH unit. Table 1 contains the slope values calculated. Correlation coefficients were all greater than 0.996.

X-ray powder diffraction analysis

Air-dried samples were ground in an agate mortar to a particle size of less than 44 μm dia. (to pass No. 325 mesh screen) and packed in an aluminum holder. The specimens were analyzed with a standard Norelco X-ray diffraction unit using Mn-filtered Fe K–α radiation generated at 35 kV and 14 mA.

Infrared analysis

Air-dried samples were ground in an agate mortar to a particle size of less than 22 μm dia. (to pass No. 500 mesh screen). About 5 mg of sample were ground under acetone for 10 minutes and applied in suspension to a 2 × 4 cm Irtran-2 (Perkin–Elmer) plate and allowed to air-dry. The samples were analyzed on a Perkin–Elmer 467 i.r. Spectrophotometer operated in the double-beam mode.

Iron analysis

The aqueous iron concentration of those samples with pH values less than 3.5 were determined. After suspended matter was removed by centrifuging and decanting a portion of the liquid, the aqueous iron was complexed with 1.10 orthophenanthroline (American Public Health Association, 1971), and the concentration of the complex determined using a Bausch–Lomb Spectronic 20 Colorimeter operated at 420 nm wavelength.

Table 1. Titration slope values in 10^2 μM/g·pH unit

Solution	Time (days) 1	2	4	7	15	30	60	120
B	2.48	2.33	2.29	2.22	2.20	2.17	2.10	1.84
C	2.65	2.92	2.52	1.95	2.36	2.35	2.35	1.97
D	2.78	2.53	2.49	2.10	2.22	2.26	2.16	1.88
E	2.82	2.82	2.45	2.31	2.07	1.97	1.90	
F	2.55	2.53	2.12	2.16	1.91	1.40	1.18	0.71
G	2.14	2.00	2.02	1.84	1.76	1.40	1.10	0.76
H	1.86	1.89	1.84	1.77	1.62	1.29	1.13	0.65
I	1.88	1.75	1.52	1.53	1.31	1.23	1.13	0.53
J	1.08	1.06	1.06	0.98	0.96	0.70	0.66	0.52

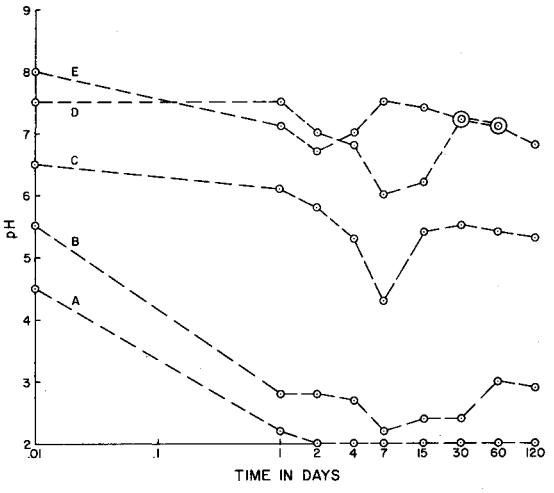


Figure 1. Variation of pH with time for suspension A–E.

RESULTS

pH Variation

Several different patterns of pH change during solution ageing were observed in this study, dependent upon the initial suspension pH. The suspensions are designated by letters A–J, and pH vs time is plotted in Figures 1 and 2. Although the initial pH was measured immediately after gel precipitation and pH adjustment, it is plotted in Figures 1 and 2 at 0.01 days, approx. 15 min after gel precipitation, in order to place this important parameter on a figure with the logarithm of time as an axis.

Three different patterns of pH variation were observed in this study:

(1) a rapid initial pH drop during the first 48 hr

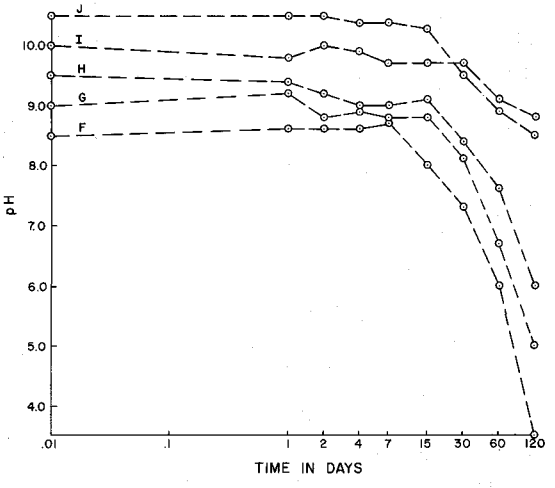


Figure 2. Variation of pH with time for suspensions F–J.

https://doi.org/10.1346/CCMN.1976.0240608 Published online by Cambridge University Press

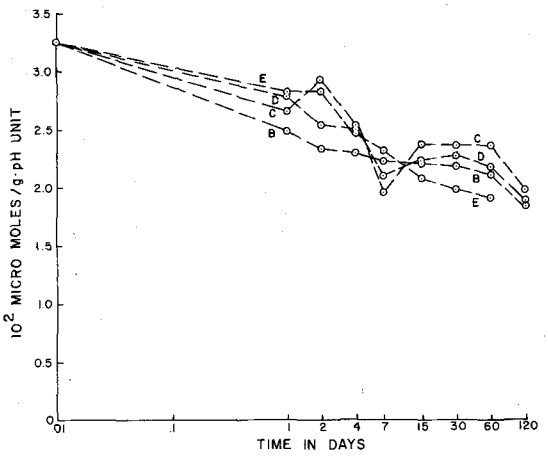


Figure 3. Variation of proton adsorption slope with time for solutions B–E.

and little pH change thereafter; (2) an initial pH drop to a minimum figure, from 2 to 7 days after precipitation, followed by a pH increase to a relative maximum, from 7 to 30 days after precipitation, and little change thereafter; and 3. little or no pH change during the first 2 weeks and then a dramatic pH decline.

The only example of the first pH variation pattern is suspension A (Figure 1). The pH of this suspension, initially at 4.5, had dropped to 2.2 after 24 hr. A pH of 2.0 was reached after 48 hr and persisted to the end of the study.

The second pH variation pattern is illustrated by suspension B–E in Figure 1. Suspensions B, C, and D, which had initial pH values of 5.5, 6.5, and 7.5, experienced pH minimums at 7 days. Suspension B pH increased to a maximum on day 60 and then declined slightly, whereas the pH of solutions C and D increased to a maximum at 30 days and then declined slightly. Suspension E, which had an initial pH of 8.0, reached a pH minimum after only 2 days, increased to a maximum at 7 days, and declined slightly thereafter.

Suspensions F–J, which illustrate in Figure 2 the third pH variation pattern, started with pH values of 8.5 or greater and did not significantly change during the first 7 days. After this time, they all experienced sharp and monotonic decreases in pH, several of them reaching pH values well below those developed at the same time by solutions that had started at lower pH.

Proton adsorption variation

The time dependence of proton adsorption slope observed in Figures 3 and 4 is highly variable. However, three basic patterns emerge from these figures: (1) continuous decline to a value of about $2 \cdot 10^2$ μM/g·pH unit; (2) erratic decline, with a minimum at 7 days, to a value of about $2 \cdot 10^2$ μM/g·pH unit; and (3) continuous decline to a value of about $8 \cdot 10^2$ μM/g·pH unit.

After 24 hr there remained no precipitate in suspension A. The dissolution of the precipitate was undoubtedly due to the low pH developed in this suspension. Since no precipitate developed during the remainder of the study, no proton adsorption data was generated from this suspension, and thus none appears on Figures 3 and 4.

Suspensions B–E all approached the same final adsorption slope but before the final value was reached the samples displayed considerable variation in aging pattern. Because of the low pH, expression of adsorption slope for suspension B on a per gram of suspended solid basis required determination of the suspended iron present. Analysis for dissolved iron in suspension B indicated that about 10% of the total iron was in dissolved form, thus allowing calculation of suspended iron concentration and adjustment of surface charge titration data to a per gram basis. After mathematical adjustment was made for the actual concentration of suspended solid in sample B, the adsorption slopes of samples B and E both declined continuously during the study.

In contrast to the simple variation pattern for the adsorption slope values for suspensions B and E, the slope values for suspensions C and D changed dramatically with time. The slope value for suspension C reached a maximum value after 2 days and then declined to a minimum at 7 days. A sharp increase in this parameter was then observed at 15 days, followed by a gradual decline to the end of the study. The adsorption slope variation for suspension D was similar to suspension C; a minimum was reached at 7 days, followed by a sharp increase at 15 days, and gradual decline thereafter.

Suspensions F–J showed nearly continuous decline in adsorption slope value with time and the rate of initial slope decrease was greater for higher initial pH, e.g. suspension J versus H. After 120 days, all five suspensions had reached approximately the same slope value, $8 \cdot 10^2$ μM/g·pH unit.

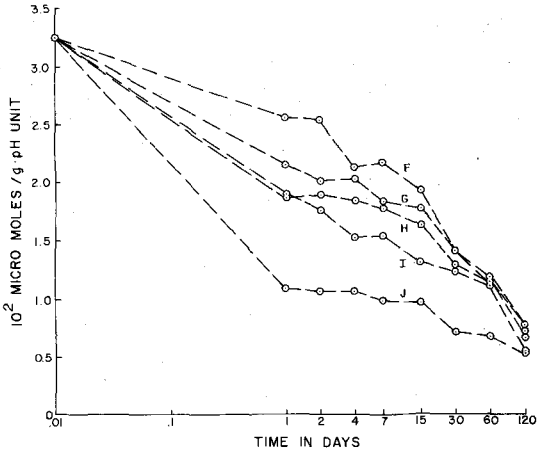


Figure 4. Variation of proton adsorption slope with time for solutions F–J.

https://doi.org/10.1346/CCMN.1976.0240608 Published online by Cambridge University Press

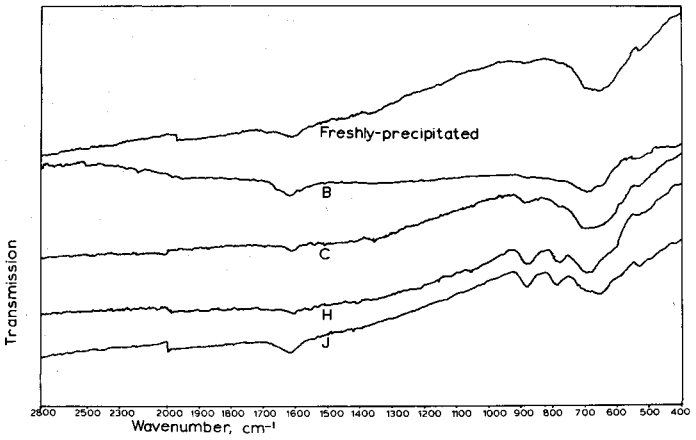


Figure 5. Infrared spectra for freshly precipitated ferric hydroxide precipitate and for suspensions B, C, H, and J after 60 days.

X-ray and infrared analysis

Because all solids were X-ray amorphous, infrared spectroscopy was used to follow changes in crystallinity. Infrared adsorption patterns for freshly precipitated ferric hydroxide indicated that it was amorphous (Figure 5). The solids in suspension B remained amorphous throughout the study. Those in suspensions C, D, and E developed small goethite adsorption bands at 795 and 890 cm^{-1} (Landa and Gast, 1973) during the first week, and these bands persisted without change throughout the lifetime of these samples (Figure 5). The goethite adsorption bands became progressively stronger with time for suspensions F–J, and for solutions of equal age they were stronger for the suspension with the higher initial pH.

DISCUSSION

All of the suspensions studied decreased in pH after preparation, solution F showing the greatest variation (Figure 2). The most likely cause of this acid production is the replacement of Cl^- ions by OH^- ions in the coordination sphere of the ferric ion, as shown by equation (1):

$$Fe(OH)_2Cl \cdot 3H_2O + OH^- \rightarrow Fe(OH)_3 \cdot 3H_2O + Cl^-. \quad (1)$$

This conclusion is consistent with the findings of Fripiat and Pennequin (1965) who found that Cl^- ions were still being expelled from a ferric hydroxide gel, prepared from ferric chloride solution, after 7 days of dialysis.

If 2–3% of the ferric ions present in the sample reacted as in equation (1), the observed pH variation could be accounted for.

Suspensions A and F–J demonstrated significantly greater acid production than did suspensions B–E. In the case of suspension A, dissolution of the precipitate resulted in contact between bulk solutions and all ferric ions, leading to greater ligand exchange. The greater acid production of suspensions F–J is consistent with the observed variations in surface charge between these suspensions and suspensions B–E. After 120 days, suspensions F–J contained only about one third the titratable charge present in suspensions B–E, suggesting a significantly greater degree of surface area reduction, and presumably expulsion of Cl^- from the precipitate as a result of goethite formation, as indicated by infrared spectroscopy (Figure 5).

The data in Figures 3 and 4 clearly demonstrate that proton adsorption slopes varied both significantly and systematically with time and solution pH in this study. Two major characteristics may be observed immediately:

1. those suspensions with initial pH greater than 8.0 showed significantly greater surface charge reduction than those suspensions with lower initial pH values (suspensions B–E);

2. initial suspension pH dramatically increased the initial rate of surface charge reduction for suspensions F–J.

Based on the work of Parks (1965), the zpc of the precipitates in this study was probably between 6 and 8. As the pH dropped for suspensions F–J, the charge/unit area declined, since the suspension pH was approaching the zpc. Only after crystallization (as determined by infrared spectroscopy) had progressed for 60 days did any of these suspensions develop a pH below 7. Thus during the early stages of crystallization, suspensions pH variations would have favored increased particle associations.

Since both observed solution pH change and crystallization of the gel would act to reduce the amount of titratable surface charge, one would predict a continuous decline in the proton adsorption slope with time, as is observed in Figure 4.

The initial rate of surface charge reduction for suspensions F–J (Figure 4) was related to initial suspension pH (Figure 2); the higher the initial pH, the greater the initial rate of charge reduction. The convergence of the slopes of suspensions F–J with time suggests the presence of a stable end product which

https://doi.org/10.1346/CCMN.1976.0240608 Published online by Cambridge University Press

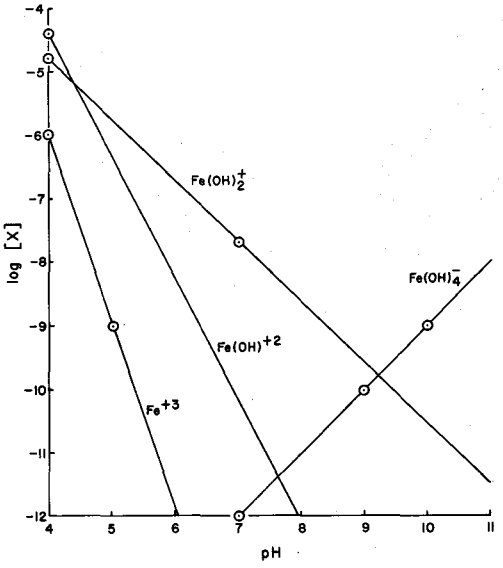


Figure 6. Solubility of ferric oxy-hydroxo species in equilibrium with amorphous ferric hydroxide (modified from Black, 1967).

is more rapidly attained at higher pH. Suspensions F–J developed infrared adsorption patterns characteristic of goethite which is thought to form from amorphous ferric hydroxide by dissolution and reprecipitation (Fischer and Schwertmann, 1975). The increased rate of surface charge reduction with pH would suggest that dissolution and reprecipitation occurs more rapidly at high pH. Thermodynamic data was used to construct Figure 6 (modified from Black, 1967), which indicates the concentration of aqueous ferric-hydroxy species in equilibrium with amorphous ferric hydroxide as a function of pH. The pH range in Figure 6 in which $Fe(OH)_4^-$ is the most soluble ferric oxyhydroxide species, 9.3 or greater, corresponds rather well with the initial pH range, 8.5 or greater, for those suspensions which showed the greatest surface charge reduction and which developed goethite infrared adsorption patterns. Further, as initial pH increased above 8.5, the initial rate of surface charge reduction increased (Figure 4) which corresponds in Figure 6 to the increased solubility of $Fe(OH)_4^-$. The probable cause for the more rapid initial rate of surface charge reduction with pH in suspensions F–J, therefore, is the increased solubility of $Fe(OH)_4^-$, which serves to transport ferric ions from the more soluble amorphous gel to the surface of the growing goethite crystal.

Although suspensions B–E converged on approximately the same titration slope value (Figure 3), the variation in adsorption slope and pH (Figure 1) with time was much more complex for these samples than was observed for suspensions F–J. Suspension E, whose pH ranged from 8.0 to 6.7, was apparently in the range of approximately neutral surface charge throughout its lifetime, whereas suspension B, whose pH ranged from 5.5 to 2.2, was always in a pH region where the gel had a high positive surface charge. One would predict, based on surface charge considerations, that both of these suspensions should show continuous surface charge reduction. This prediction is verified in Figure 3. Despite the differences in surface charge and suspension pH, the adsorption slope for both suspensions declines continuously to about the same value. This phenomenon suggests that whatever mechanism is responsible for the adsorption slope reduction, it is not dependent on reactions involving the particle surface or bulk solution.

Suspensions C and D had initial pH values near the expected zpc for the precipitate. Figure 1 shows, however, that within the first 7 days the pH for suspension C declined into the region associated with positive charged particles. Based on surface charge considerations, one would predict that this pH variation would induce greater particle–particle repulsions and increase the surface area of the solid. The proton adsorption slope (Figure 3) for this sample did increase, but the increase was not coincident with the pH minimum, but occurred at 15 days when the pH had moderated. Apparently the increase in surface area is not immediate, but requires time to develop. The rise in pH associated with the rise in adsorption slope is probably due to proton adsorption from the solution as "new" surface is exposed to bulk solution at a lower pH.

The pH variation observed for sample D (Figure 1) was within the range associated with the zpc for the precipitate. Based on this observation, one would predict a continuous decline in proton adsorption slope with time. Figure 3 illustrates, however, that sample D displays an adsorption slope behavior very similar to sample C, although not quite so erratic. Apparently some dispersion of the material has occurred, although from the minimum pH recorded this would not have been predicted. Either the zpc for the solid is nearer to 8 than 6 or some other phenomenon has occurred in the sample to account for the increased adsorption slope.

The convergence with time of the proton adsorption slope values for the four suspensions, B–E, despite markedly different histories, suggests that the causative mechanisms for the surface charge reduction was internal rearrangement. This observation is consistent with the findings of Fisher and Schwertmann (1975) that hematite is formed from amorphous ferric hydroxide by "internal dehydration." Although no evidence of hematite formation was found, these precipitates were maintained in the pH region found by other authors to favor hematite formation. The 50% reduction in surface charge indicates that some reorganization of the precipitate had occurred.

CONCLUSIONS

It has been shown that variation in the proton adsorption slope of ferric hydroxide precipitates with time may be used to monitor changes occurring in the precipitate, and that in most cases if the pH vari-

https://doi.org/10.1346/CCMN.1976.0240608 Published online by Cambridge University Press

ation of the sample is known, the proton adsorption slope variation may be predicted. Identical precipitates aged in solutions of different pH developed different crystallization products which could be differentiated on the basis of proton adsorption slope and infrared adsorption patterns. The pH dependence of adsorption slope reduction was found to be consistent with the findings of Fischer and Schwertmann (1975) on the mechanisms of goethite and hematite formation from ferric hydroxide.

Acknowledgements—The author would like to gratefully acknowledge the assistance of Dr. D. L. Graf of the Department of Geology, University of Illinois, who supervised the research and Dr. Herman Roberson, Department of Geological Sciences, State University of New York at Binghamton, who reviewed the manuscript.

REFERENCES

American Public Health Association (1971) *Standard Methods for the Examination of Waste and Wastewater*, 13th Edn., APHA, New York.

Atkinson, R. J., Posner, A. M. and Quirk, J. P. (1967) Adsorption of potential-determining ions at the ferric oxide–aqueous electrolyte interface: *J. Phys. Chem.* **71,** 550–558.

Black, A. P. (1967) Electrokinetic characteristics of hydrous oxides of aluminum and iron in *Principles and Applications of Water Chemistry* (Edited by Faust, S. D. and Hunter, J. V.). Wiley, New York.

Fischer, W. R. and Schwertmann, U. (1975) The formation of hematite from amorphous iron (III) hydroxide: *Clays & Clay Minerals* **23,** 33–37.

Fripiat, J. J. and Pennequin, M. (1965) Évolution de la composition et du poids moléculair des hydroxydes d'aluminium et de fer purifiés par dialyse: *Bull. Soc. chim. Fr.* **244,** 1655–1660.

Gastuche, M. C. (1964) The octahedral layer: 12*th Nat. Cong. Clays & Clay Mins.*, pp. 471–493.

Gastuche, M. C., Bruggenwert, T. and Mortland, M. M. (1964) Crystallization of mixed iron and aluminum gels: *Soil Sci.* **98**(5), 281–289.

Hingston, F. J., Atkinson, R. J., Posner, A. M. and Quirk, J. P. (1968) Specific adsorption of anions on goethite: 9*th. Int. Con. Soil. Sci. Trans.*, pp. 669–667.

Landa, E. R. and Gast, R. G. (1973) Evaluation of crystallinity in hydrated ferric oxides: *Clays & Clay Minerals* **21,** 121–130.

MacKenzie, R. C. (1957) *The Differential Thermal Investigation of Clays.* Mineralogical Society, London.

MacKenzie, R. C. and Meldau, R. (1959) The aging of sesquioxide gels—I. Iron oxide gels: *Mineralog. Mag.* **32,** 153–165.

Parks, G. A. (1965) The isoelectric points of solid oxides, solid hydroxides and aqueous hydroxo complex systems: *Chem. Rev.* **65,** 177–198.

Parks, G. A. (1967) Aqueous surface chemistry of oxides and complex oxide minerals. *Equilibrium Concepts in Natural Water Chemistry* (Edited by Gould, R. F.). Adv. Chem. Ser. 67.

Parks, G. A. and DeBruyn, P. L. (1962) The zero-point-of-charge of oxides: *J. Phys. Chem.* **66,** 967–973.

Schellman, W. (1959) Experimentelle Untersuchungen über die sedimentaire bildung von Goethite und Hematit: *Chemie Erde* **20,** 104–135.

Schwertmann, U. (1969) Die Bildung von Eisenoxidmineralen: *Fortschr. Miner.* **46,** 274–285.

Schwertmann, U. and Fischer, W. R. (1966) Zur Bildung von α-FeOOH und α-Fe_2O_3 aus amorphen Wisen (III)-hydroxide: *Z. anorg. allg. Chem.* **346,** 137–142.

Schwertmann, U. and Fischer, W. R. (1973) Natural 'amorphous' ferric hydroxide: *Geoderma* **10,** 237–247.

https://doi.org/10.1346/CCMN.1976.0240608 Published online by Cambridge University Press